VIP Cyclopentadienyl Complexes

DOI: 10.1002/anie.200705001

Remarkable Stability of Metallocenes with Superbulky Ligands: Spontaneous Reduction of Sm^{III} to Sm^{II}**

*Christian Ruspic, John R. Moss, Markus Schürmann, and Sjoerd Harder**

Complexes containing extremely bulky ligands such as the perphenylated cyclopentadienyl ligand (Ph_5C_5) have shown unique properties or coordination geometries.[1] For example, the typical bent structures of the carbene analogue decamethylstannocene ([$Cp^*_2Sn^{II}$], $Cp^* = C_5Me_5$) can be linearized by use of Ph_5C_5 ligands.[2] Surprisingly, the nickelocene complex [$(Ph_5C_5)_2Ni$], prepared by reaction of the $Ph_5C_5^{\bullet}$ radical with a Ni^0 derivative, is diamagnetic.[3] The existence of [$(Ph_5C_5)_2Fe$] was long disputed on the basis of its short ring–ring distance.[4] Today, two linkage isomers are known: the more sterically relaxed zwitterionic η^5,η^6-complex **1**[5] and the sterically congested (η^5,η^5)-metallocene **2**.[6]

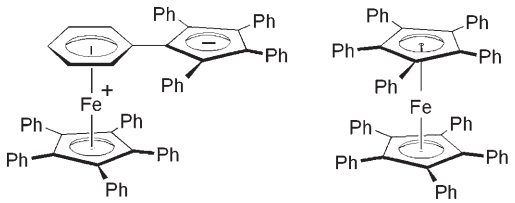

1 **2**

First reports on the use of the Ph_5C_5 ligand in catalysis show that it greatly enhances stereoselectivity in asymmetric syntheses.[7] Moreover, the bulk of the ligand increases the activity and selectivity in chromium-catalyzed ethylene oligomerization.[8] As half-sandwich complexes of alkaline-earth and lanthanide metals are effective and promising catalysts for a wide variety of applications,[9] we pursued the introduction of superbulky cyclopentadienyl ligands in these compound classes. Our surprising initial results show that instead of half-sandwich complexes, generally sterically congested metallocenes are formed.

Complexes containing the Ph_5C_5 ligand are very insoluble on account of their rigidity and high symmetry.[1] Therefore, we used the modified perarylated cyclopentadiene (4-*n*Bu-$C_6H_4)_5C_5H$ ($Cp^{BIG}H$), which can be obtained in a simple high-yield, one-pot procedure.[10] This ligand can be smoothly deprotonated by [(4-*t*Bu-benzyl)$_2$(thf)$_4$Ca] in benzene at 60 °C (Scheme 1). However, instead of heteroleptic [(Cp^{BIG})(4-*t*Bu-benzyl)Ca], the calcocene [$(Cp^{BIG})_2$Ca] was isolated as large yellow crystals that are readily soluble in hexane (43 % yield based on $Cp^{BIG}H$). Despite the bulkiness of the Cp^{BIG} ligand, the Schlenk equilibrium is apparently at the homoleptic side. Reactions of [$(Cp^{BIG})_2$Ca] with [(4-*t*Bu-benzyl)$_2$(thf)$_4$Ca] or [(2-Me_2N-α-Me_3Si-benzyl)$_2$(thf)$_2$Ca] both gave no ligand exchange, which implies high stability of the calcocene.[11]

Reaction of equimolar amounts of $Cp^{BIG}H$ with [(2-Me_2N-benzyl)$_3$Y] in benzene (Scheme 2) gave the half-sandwich complex [(Cp^{BIG})(2-Me_2N-benzyl)$_2$Y] as colorless needlelike crystals (yield: 31 %). However, the analogous reaction with [(2-Me_2N-benzyl)$_3$Yb] resulted in spontaneous reduction to the Yb^{II} metallocene [$(Cp^{BIG})_2$Yb], which crystallized as dark green blocks (yield: 22 %; the yield could be increased to 36 % by using the correct 2:1 stoichiometry).

Spontaneous reduction of Ln^{III} ions (Ln = lanthanide) is easily accomplished for Eu (Eu^{3+}/Eu^{2+} $E_{1/2} = -0.35$ V)[12] and has been observed on several occasions.[13] Reduction of Yb^{III} is less favorable (Yb^{3+}/Yb^{2+} $E_{1/2} = -1.15$ V)[12] but has been observed before; decomposition of the dimer [{$(MeH_4C_5)_2$YbMe}$_2$] to the Yb^{II} metallocene in toluene is an extraordinarily slow reaction [Eq. (1)].[14] Reaction times can be reduced substantially by addition of diethyl ether as a coordinating solvent (50 % conversion is observed after 8 h at 80 °C in a pressure vessel).[14] The importance of Lewis bases is underscored by a more recent example of spontaneous Yb^{III} reduction. Reaction of [{$(Me_3Si)_2N$}$_3$$Yb^{III}$] with two equivalents of indene gave the expected Yb^{III} product [Eq. (2)]. Reaction with an indene derivative containing chelating Me_2N arms, however, gave exclusively reduction of the metal [Eq. (3)].[15] Although it is unclear why the presence of coordinating Lewis bases results in spontaneous reduction of Yb^{III}, a suitable working hypothesis could be that the Yb^{II} metal in the product has a larger ionic radius, thus allowing for energetically favorable coordination of additional Lewis bases (for eight-coordinate species: Yb^{2+} 1.14, Yb^{3+} 0.985 Å).[16]

Encouraged by these results, we investigated the reaction of [(2-Me_2N-benzyl)$_3$Sm] with $Cp^{BIG}H$. In this case as well, a reduction of Sm^{III} is observed. The samarocene [$(Cp^{BIG})_2$Sm], with the metal in its highly reactive 2+ oxidation state, was

[*] C. Ruspic, Prof. Dr. S. Harder
Anorganische Chemie, Universität Duisburg-Essen
Universitätsstrasse 5, 45117 Essen (Germany)
Fax: (+49) 201-183-2621
E-mail: sjoerd.harder@uni-due.de
Prof. Dr. J. R. Moss
Department of Chemistry, University of Cape Town
Rondebosch 7701, Cape Town (South Africa)
Dr. M. Schürmann
Anorganische Chemie, Universität Dortmund
44221 Dortmund (Germany)

[**] S.H. kindly acknowledges the University of Cape Town for an extensive research stay in the autumn of 2003. We are grateful to the DFG for financial support (SPP1166: "lanthanide-specific functionalities in molecule and material") and acknowledge Prof. Dr. Boese and D. Bläser for collection of X-ray data and H. Bandmann for measurement of 500 MHz NMR spectra.

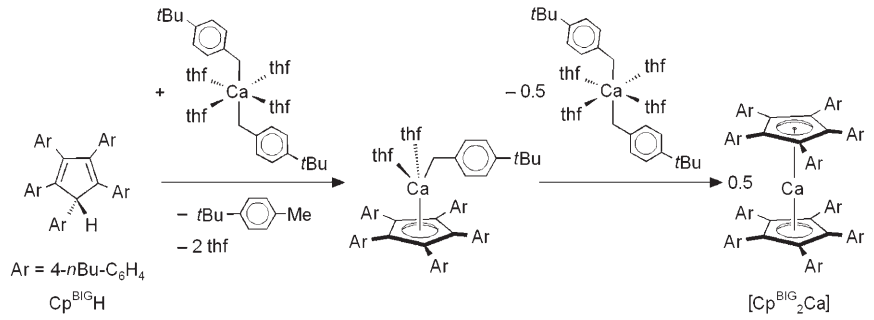

Scheme 1. Reaction of $Cp^{BIG}H$ with a dibenzylcalcium derivative.

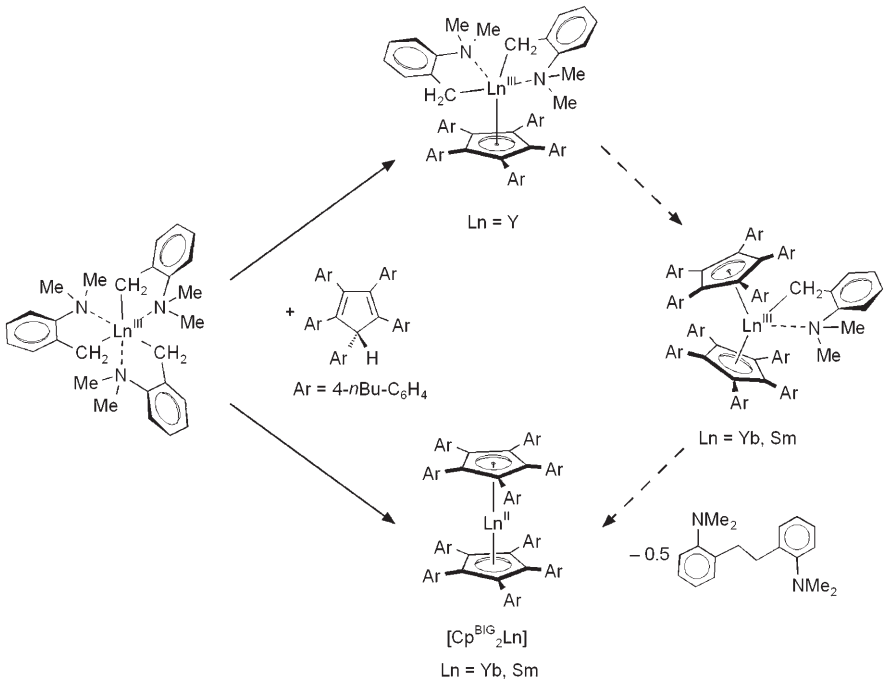

Scheme 2. Reactions of $Cp^{BIG}H$ with benzyllanthanide derivatives.

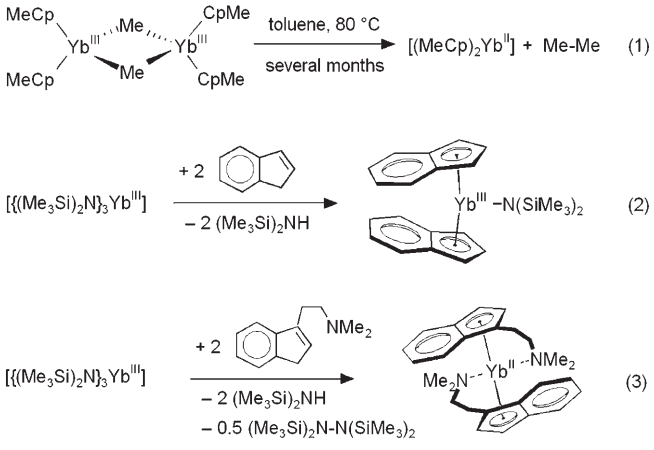

isolated in the form of red-brown crystals (36% yield). The instability of Sm^{II} against oxidation is well-known (Sm^{3+}/Sm^{2+} $E_{1/2} = -1.55$ V).[12] SmI_2 is used as a versatile reducing agent in organic chemistry,[17] and $[Cp^*_2Sm]$ is even able to reduce molecular nitrogen.[18] In this light, the spontaneous reduction of a Sm^{III} precursor to the samarocene $[(Cp^{BIG})_2Sm^{II}]$ is remarkable.

The exact mechanism for this reduction is unclear. In analogy to the reaction with yttrium described above (Scheme 2), the first step could be formation of the half-sandwich complex $[(Cp^{BIG})(2\text{-}Me_2N\text{-benzyl})_2Ln]$. This complex could be converted to $[(Cp^{BIG})_2(2\text{-}Me_2N\text{-benzyl})Ln]$ either by reaction with $Cp^{BIG}H$ or by ligand exchange. Steric crowding in the latter intermediate could give spontaneous reduction to the metallocene $[(Cp^{BIG})_2Ln]$ and a 2-Me_2N-benzyl radical. This proposed mechanism is confirmed by detection of 1,2-di(2-Me_2N-phenyl)ethane as a major side product in the mother liquors. The mechanism is also supported by the well-established sterically induced reduction chemistry (SIR)[19] that has been discovered by the pioneering work of Evans et al. on sterically overloaded $[Cp^*_3Sm]$.[20] The latter complex shows the same redox reactivity as $[Cp^*_2Sm]$ (Scheme 3).[21] The performance of $[Cp^*_3Sm]$ as a reducing agent has been explained by oxidation of the Cp* anion. The spontaneous reduction of Sm^{III} described herein might shed light on the mechanism of SIR and suggests that instead of intermediate $[Cp^*_2Ln^{III}]^+$, transient Ln^{II} species could also play a role. In this respect, Lappert and co-workers' spectroscopic and synthetic evidence for La^{II} complexes should be noted.[22]

Considering the bulk of the Cp^{BIG} ligand, it seems reasonable to assume that the spontaneous reduction of Sm^{III} in $[(Cp^{BIG})_2(2\text{-}Me_2N\text{-benzyl})Sm^{III}]$ is driven by steric congestion. On the other hand, $[(\eta^3\text{-}Ph_5C_5)_2W{=}O]$, a complex with a much smaller metal, has been characterized by X-ray diffraction.[23] Therefore, the driving force for the lanthanide reduction in Scheme 2 could also be partly due to the higher basicity and thus easier oxidation of the benzyl anion compared to the Cp* anion. In this respect, it should be mentioned that a recent new preparative method for $[Cp^*_3Sm]$ is based on the reverse of SIR, that is, oxidation of $[Cp^*_2Sm]$ by reduction of Cp*–Cp* [Eq. (4)].[24] This result implies that the first step in SIR of $[Cp^*_3Sm]$ is an equilibrium that is largely on the side of $[Cp^*_3Sm]$.

$$2\,[Cp^*_2Sm^{II}] + Cp^*\text{–}Cp^* \xrightarrow[80\,^\circ C]{\text{benzene}} 2\,[Cp^*_3Sm^{III}]\ (84\,\%) \qquad (4)$$

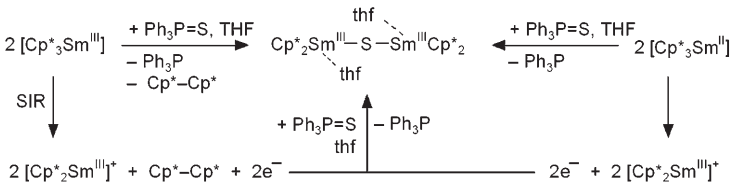

Scheme 3. Reduction of $Ph_3P{=}S$ by either [Cp*$_3$Sm] (SIR) or [Cp*$_2$Sm].[21]

Another important driving force for spontaneous Ln^{III} reduction could be the remarkable stability of the metallocene complex $[(Cp^{BIG})_2Ln]$ itself. Although formation of these sterically congested complexes might not seem favorable at first sight, more detailed investigations of their crystal structures shed light on their unusual stability.

The metallocenes $[(Cp^{BIG})_2M]$ (M = Ca, Yb, Sm) crystallize isomorphously in space group $P\bar{1}$ with the metal ion on the center of inversion (Figure 1). Considering the presence of many *n*-butyl substituents, the structures are surprisingly ordered and of good quality. The propeller-like ligands have opposite chirality and interlock like a gear box. The metals are bound in nearly perfect η^5,η^5 fashion (Table 1). However, it should be mentioned that for the heavier metals unusually high displacement factors parallel to the ring planes are observed (Figure 1 b). This anisotropy, which is not as distinct in the calcocene, is especially noteworthy in the samarocene (despite measurement at a lower temperature). As heavier alkaline-earth and Ln^{II} metallocenes typically exhibit unusually bent structures,[25] this anisotropy might be explained by assuming that the metals are slightly disordered within a plane parallel to the Cp rings. Consequently, a structure with parallel ligands but with a bent Cp_{center}-M-Cp_{center} unit results (Scheme 4). This implies that there is some deviation from η^5 coordination. Parallel ligands but bent C-M–C bonds have also been observed in $[\{(Me_3Si)_3C\}_2Ca]$.[26]

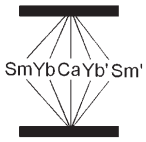

Scheme 4.

The average M–C bonds in $[(Cp^{BIG})_2M]$ (Table 1) compare remarkably well to those in the analogous $[Cp^*_2M]$ complexes (Ca 2.64(1),[25b] Yb 2.665(3),[25f] Sm 2.79(1) Å[25g]). As the latter metallocenes are bent and the Cp* ligand differs substantially from the Ar_5C_5 ligand,[27] this agreement is merely coincidental. Comparison of the average Yb–C bond length in $[(Cp^{BIG})_2Yb]$ (2.673(2) Å) with that in the only other Ar_5C_5 complex of a lanthanide or alkaline-earth metal, $[\{(\eta^5\text{-}Ph_5C_5)Yb(\mu\text{-}C{\equiv}CPh)(thf)\}_2]$ (2.726(7) Å),[28] led us to conclude that the Cp–M bond in $[(Cp^{BIG})_2Yb]$ is unexpectedly short.[29]

One feature in particular could contribute to the unusual stability of $[(Cp^{BIG})_2M]$ complexes. In all three structures, short distances between an *ortho* H atom of one ligand and an *ortho* C atom of the other ligand are evident (Figure 2). These merry-go-round interligand contacts are in all $[(Cp^{BIG})_2M]$ complexes considerably shorter than the sum of the van der Waals radii for C and H (2.90 Å), thus indicating C–H···C(π) hydrogen bonds. Average values are 2.68(1) (M = Ca), 2.74(2) (M = Yb), and 2.78(2) Å (M = Sm); aryl H atoms have been refined. These contacts are even shorter when more realistic (neutron-diffraction-like) calculated hydrogen positions with a fixed C–H distance of 1.08 Å are used (Table 1).[30] The observed H···C contacts are of comparable length to C–H···C(Cp^-) interactions in salts $[R_4P^+][Cp^-]$ containing the "naked" Cp anion.[31e] Concomitant large C–H···C angles (Table 1) indicate an energetically favorable interaction. Such nonclassical hydrogen bonds, arising from

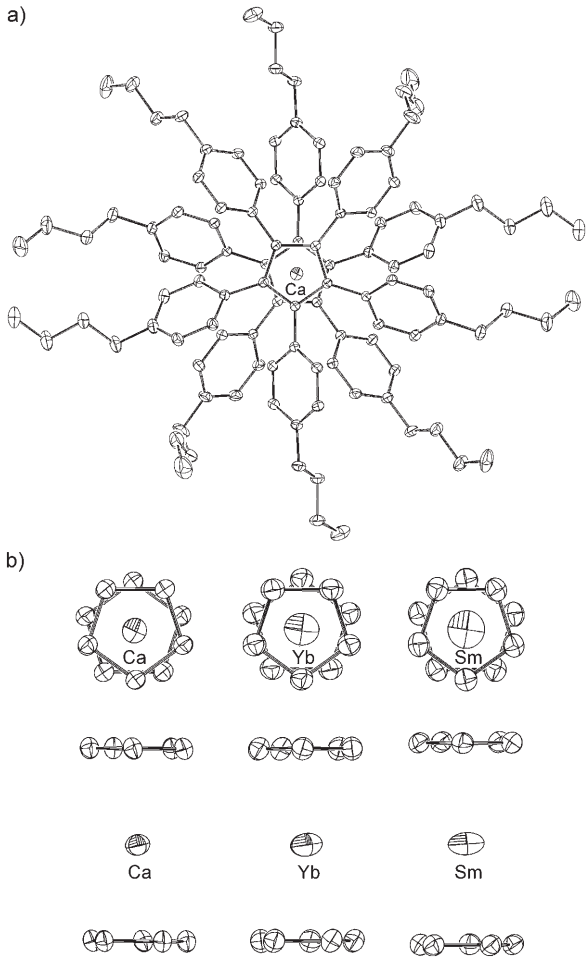

Figure 1. a) Crystal structure of $[(Cp^{BIG})_2Ca]$ (ORTEP with thermal ellipsoids set at 30% probability). Hydrogen atoms have been omitted for clarity. b) ORTEP representations (top and side views with thermal ellipsoids set at 50% probability) for partial structures of $[(Cp^{BIG})_2Ca]$ (−70 °C), $[(Cp^{BIG})_2Yb]$ (−70 °C), and $[(Cp^{BIG})_2Sm]$ (−100 °C).

interaction of a $C^{\delta-}$–$H^{\delta+}$ dipole with the aryl π system, are well-established[31] and explain the typical "herringbone" structure in crystalline benzene (Scheme 5).[32] The perpen-

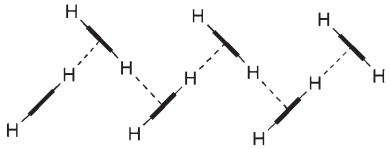

Scheme 5.

Table 1: Geometrical data for centrosymmetric metallocenes with Ph_5C_5 or Cp^{BIG} ligands (sorted in order of increasing metal size).[a]

Complex	M–Cp_{center}	M–C	C_{ipso}–C_{Cp} ⊥ Cp[b]	H···C[c]	C–H···C[c]
$[(Ph_5C_5)_2Fe]$[6]	1.724(8)	2.04(2)–2.19(2)	+7.8(11)/+13.9(18)	2.34–2.50	162–177
		[2.12(2)]	[+11.4(13)]	[2.41]	[173]
$[(Ph_5C_5)_2Ni]^+$[35]	1.839(2)	2.188(5)–2.229(5)	+3.8(4)/+12.0(4)	2.39–2.47	144–177
		[2.204(5)]	[+8.4(13)]	[2.43]	[167]
$[(Ph_5C_5)_2Cr]^+$[36]	1.932(3)	2.268(5)–2.302(5)	+5.9(4)/+8.9(4)	2.41–2.51	149–179
		[2.281(5)]	[+7.2(4)]	[2.45]	[168]
$[(Ph_5C_5)_2W]^+$[37]	2.018(2)	2.345(6)–2.371(6)	+5.1(4)/+7.5(4)	2.45–2.53	169–175
		[2.357(6)]	[+6.2(4)]	[2.49]	[171]
$[(Cp^{BIG})_2Ca]$	2.3561(4)	2.643(1)–2.661(1)	+0.031(6)/−2.31(6)	2.51–2.65	153–159
		[2.651(1)]	[−1.21(6)]	[2.58]	[155]
$[(Cp^{BIG})_2Yb]$	2.382(1)	2.666(2)–2.679(2)	+0.03(1)/−2.7(1)	2.54–2.67	152–158
		[2.673(2)]	[−1.4(1)]	[2.61]	[154]
$[(Ph_5C_5)_2Sn]$[2]	2.401(3)	2.686(7)–2.705(7)	+0.6(4)/−2.6(4)	2.63–2.77	150–164
		[2.691(7)]	[−1.2(4)]	[2.68]	[160]
$[(Cp^{BIG})_2Sm]$	2.5050(8)	2.779(2)–2.791(2)	−2.0(1)/−4.1(1)	2.61–2.74	152–158
		[2.782(2)]	[−3.5(1)]	[2.67]	[154]

[a] Distances are given in Å, angles in degrees, and average values between square brackets. [b] C_{ipso}–C_{Cp} ⊥ Cp represents the angle between the C_{ipso}–C_{Cp} vector and the least-squares plane of the Cp ring (± values define bending away/towards the metal, see Scheme 7). [c] H···C represents the shortest contact between the aryl rings of one ligand and those of the other ligand (see Figure 2). For better comparison of all structures, the hydrogen atoms have been set at realistic positions with C–H bonds of 1.08 Å.

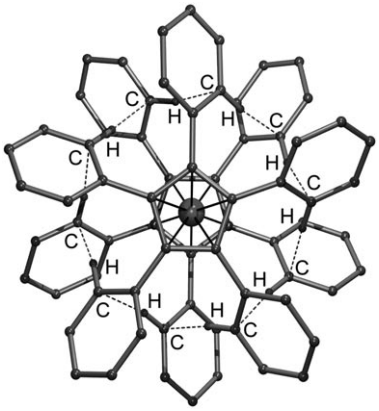

Figure 2. Partial structure of $[(Cp^{BIG})_2Ca]$ showing the merry-go-round C–H···C(π) hydrogen-bond network. Similar structures are observed for $[(Cp^{BIG})_2Yb]$ and $[(Cp^{BIG})_2Sm]$.

dicular orientation of the aryl rings in $[(Cp^{BIG})_2M]$ complexes is an S_{10}-symmetric circular version of this herringbone structure.

Although never discussed earlier, these short C–H···C(π) hydrogen bonds are even more evident in the structures of $[(Ph_5C_5)_2M]$ complexes with much smaller metals. Entries in Table 1 are sorted in order of increasing metal size and contain data for structures in which, for comparison, the C–H bonds have been set at a value of 1.08 Å. The crystal structure of $[(Ph_5C_5)_2Fe]$, which unfortunately is of poor quality, shows extremely short H···C contacts that average 2.41 Å and are of a similar value to the H···C interaction in the coordination complex [2-butyne·$(HCl)_2$] (Scheme 6).[33] This complex, with a very acidic hydrogen-bond donor (HCl) and an electron-rich acceptor (alkyne), is generally seen as the extreme in X–H···C bonding.

As expected, the interligand H···C distances in $[(Ar_5C_5)_2M]$ complexes increase with increasing metal size. However, this increase is much smaller than the increase in the ring–ring distance (which equals circa twice the M–Cp_{center} distance). This difference originates from bending of the aryl substituents out of the Cp plane (Scheme 7). The phenyl substituents in $[(Ph_5C_5)_2Fe]$ strongly bend away from the metal (average +11.4(13)°). This bending angle decreases with increasing metal size. The aryl substituents in $[(Cp^{BIG})_2Sm]$ even bend towards the metal (average −3.5(1)°). This atypical distortion is additional proof for these attractive C–H···C(π) interactions. Although the energy involved in the H···C contact is estimated to be 2–5 kcal mol^{-1},[31] the overall effect could be considerable. First of all, the molecule contains ten such contacts, and secondly, cooperative effects[34] enforce this interaction: the C–H hydrogen-bond donor also functions as the acceptor, thus increasing acidity and hydrogen-donor ability of this C–H unit.

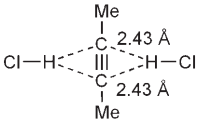

Scheme 6.

In summary, contrary to expectation, $[(Ar_5C_5)_2M]$ complexes are especially stable on account of a C–H···C(π) hydrogen-bond network that propagates through the metallocene. The high stability of these metallocenes is expressed by the spontaneous reduction of a Sm^{III} precursor to the samarocene $[(Cp^{BIG})_2Sm]$. As this modified metallocene and its analogues are readily soluble in chemically inert solvents such as hexane and crystallize isomorphously for a variety of metal sizes, the Cp^{BIG} ligand will be well-suited for capturing hitherto unknown highly reducing metals in low oxidation states. Further exploration of this intriguing ligand in the chemistry of low-valent metals is in progress.

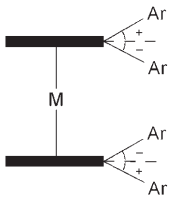

Scheme 7.

Experimental Section

All experiments were carried out under argon using standard Schlenk techniques and freshly dried, degassed solvents. The following compounds have been prepared according to the literature: (*n*Bu-$C_6H_4)_5CpH$ (= $Cp^{BIG}H$),[10] $[(4\text{-}t\text{Bu-}C_6H_4CH_2)_2(thf)_4Ca]$,[38] K[2-$Me_2$N-benzyl)][39] and $[(2\text{-}Me_2N\text{-benzyl})_3Y]$.[40]

$[(Cp^{BIG})_2Ca]$: A solution of $[(4\text{-}t\text{Bu-}C_6H_4CH_2)_2(thf)_4Ca]$ (256 mg, 0.393 mmol) and $Cp^{BIG}H$ (285 mg, 0.393 mmol) in benzene (3 mL) was stirred for 30 min at 60 °C. All solvents were removed in vacuo and hexane (3 mL) was added. Slow cooling to −30 °C gave large,

light-yellow, blocklike crystals of [(Cp^{BIG})$_2$Ca] (126 mg, 43 % yield based on $Cp^{BIG}H$). Elemental analysis (%) calcd for $C_{110}H_{130}Ca$ (M_r = 1492.34): C 88.53, H 8.78; found C 88.08, H 8.62. ^{1}H NMR (300 MHz, C_6D_6, 20 °C): δ = 0.89 (t, ^3J(H,H) = 7.2 Hz, 30 H, CH_3), 1.28 (m, 20 H, CH_2), 1.53 (m, 20 H, CH_2), 2.46 (t, ^3J(H,H) = 7.2 Hz, 20 H, CH_2), 6.83 (d, ^3J(H,H) = 7.6 Hz, 20 H, aryl), 7.13 ppm (d, ^3J(H,H) = 7.6 Hz, 20 H, aryl). ^{13}C NMR (75 MHz, C_6D_6, 20 °C): δ = 14.2 (CH_3), 22.8 (CH_2), 34.2 (CH_2), 35.7 (CH_2), 124.0, 128.5, 131.9, 134.2, 140.0 ppm. M.p. 217 °C.

[(Cp^{BIG})(2-Me_2N-benzyl)$_2$Y]: [(2-Me_2N-benzyl)$_3$Y] (22.3 mg, 45.4 μmol) and $Cp^{BIG}H$ (33.0 mg, 45.4 μmol) were dissolved in benzene (0.50 mL). After heating for 18 h at 60 °C, the volatiles were removed in vacuo (25 °C, 1 Torr, 30 min). Addition of pentane (0.40 mL) to the oily residue gave crystallization of the product in the form of small colorless needles. The crystals were washed with pentane (2 × 0.40 mL). Drying under vacuo (25 °C, 1 Torr, 30 min) gave the product as a light yellow solid (15.0 mg, 31 %). ^{1}H NMR (300 MHz, C_6D_6, 20 °C): δ = 0.83 (t, ^3J(H,H) = 7.4 Hz, 15 H, CH_3), 1.20 (m, 10 H, CH_2), 1.45 (m, 10 H, CH_2), 2.02 (s, 4 H, CH_2), 2.33–2.53 (m, 22 H, CH_2 and NMe_2), 6.74 (m, 2 H, aryl), 6.85 (d, ^3J(H,H) = 8.0 Hz, 10 H, aryl), 6.88–6.99 (m, 4 H, aryl), 7.09 (m, 2 H, aryl), 7.18 ppm (d, ^3J(H,H) = 8.0 Hz, 10 H, aryl). ^{13}C NMR (75 MHz, [C_6D_6], 20 °C): δ = 14.1 (CH_3), 22.6 (CH_2), 33.5 (CH_2), 35.5 (CH_2), 47.2 (NMe_2), 48.3 (d, ^1J(^{13}C-^{89}Y) = 34.7 Hz, CH_2), 118.4, 120.7, 126.8, 127.0, 127.8, 131.1, 132.4, 134.0, 140.0, 144.9, 145.6 ppm (aryl).

[(2-Me_2N-benzyl)$_3$Yb]: A cooled solution (−50 °C) of K[2-Me_2N-benzyl] (2.08 g, 12.03 mmol) in THF (20 mL) was added to a cooled suspension (−50 °C) of $YbCl_3$ (1.12 g, 4.01 mmol) in THF (30 mL). A rapid color change from orange to dark blue was observed. The reaction mixture was allowed to warm to 20 °C and was stirred for 1 h. After centrifugation the volatiles were evaporated in vacuo (25 °C, 1 Torr, 30 min) and the residue was recrystallized from toluene/hexane (ca. 2:1) as dark blue blocks (600 mg, 26 %). The crystal structure is isomorphous to that of [(2-Me_2N-benzyl)$_3$Y].[41] Elemental analysis (%) calcd for $C_{27}H_{36}N_3Yb$ (M_r = 575.65): C 56.34, H 6.30; found C 55.98, H 6.42. M.p. 157 °C (decomp).

[(2-Me_2N-benzyl)$_3$Sm]: K[Me_2N-benzyl] (642 mg, 3.70 mmol) was treated with $SmBr_3$ (481 mg, 1.23 mmol) analogously to the reaction with $YbCl_3$. Crystallization from toluene/hexane (ca. 2:1) resulted in the formation of the product as dark red blocks (143 mg, 21 %). The crystal structure is isomorphous to that of [(2-Me_2N-benzyl)$_3$Y].[41] Elemental analysis (%) calcd for $C_{27}H_{36}N_3Sm$ (M_r = 553.0): C 58.65, H 6.56; found C 58.27, H 6.72. ^{1}H NMR (300 MHz, C_6D_6, 20 °C): δ = −1.77 (br, 18 H, NMe_2), 4.58 (br, 3 H, aryl), 7.12 (br, 3 H, aryl), 7.25 (br, 3 H, aryl), 9.80 (br, 3 H, aryl), 14.25 ppm (br, 6 H, CH_2). ^{13}C NMR (75 MHz, C_6D_6, 20 °C): δ = 39.4 (NMe_2), 44.7 (CH_2), 111.9, 122.7, 124.3, 128.7, 131.5, 154.7 ppm. M.p. 150 °C (decomp).

[(Cp^{BIG})$_2$Yb]: [(2-Me_2N-benzyl)$_3$Yb] (13.1 mg, 22.7 μmol) and $Cp^{BIG}H$ (33.0 mg, 45.4 μmol) were dissolved in benzene (0.50 mL) and heated to 60 °C for 18 h. The volatiles were evaporated in vacuo (25 °C, 1 Torr, 30 min) and the residue was dissolved in warm hexane (0.25 mL). Slow cooling to −27 °C resulted in the formation of the product as large green blocks (25.0 mg, 36 %). Elemental analysis (%) calcd for $C_{110}H_{130}Yb$ (M_r = 1625.30): C 81.29, H 8.06; found C 80.89, H 8.24. ^{1}H NMR (300 MHz, C_6D_6, 20 °C): δ = 0.89 (t, ^3J(H,H) = 7.2 Hz, 30 H, CH_3), 1.28 (m, 20 H, CH_2), 1.53 (m, 20 H, CH_2), 2.46 (t, ^3J(H,H) = 7.2 Hz, 20 H, CH_2), 6.83 (d, ^3J(H,H) = 7.6 Hz, 20 H, aryl), 7.13 ppm (d, ^3J(H,H) = 7.6 Hz, 20 H, aryl). ^{13}C NMR (75 MHz, C_6D_6, 20 °C): 14.2 (CH_3), 22.8 (CH_2), 34.2 (CH_2), 35.7 (CH_2), 124.0, 128.5, 131.9, 134.2, 140.0 ppm. M.p. 193 °C.

[(Cp^{BIG})$_2$Sm]: [(2-Me_2N-benzyl)$_3$Sm] (24.0 mg, 43.4 μmol) and $Cp^{BIG}H$ (63.1 mg, 86.8 μmol) were dissolved in benzene (0.50 mL) and heated to 60 °C for 22 h. The volatiles were evaporated in vacuo (25 °C, 1 Torr, 30 min). The residue was dissolved in hexane (0.25 mL). The product crystallized over night at room temperature in the form of dark brown blocks (25.0 mg, 36 %). Elemental analysis (%) calcd for $C_{110}H_{130}Sm$ (M_r = 1602.62): C 82.44, H 8.18; found C 82.02, H 8.31. ^{1}H NMR (300 MHz, C_6D_6, 20 °C): δ = 2.18 (t, ^3J(H,H) = 7.4 Hz, 30 H, CH_3), 3.06 (m, 20 H, CH_2), 3.88 (m, 20 H, aryl), 5.13 (t, ^3J(H,H) = 7.4 Hz, 20 H, CH_2), 11.26 (br, 20 H, aryl), 15.67 ppm (br, 20 H, aryl). ^{13}C NMR (75 MHz, C_6D_6, 20 °C): 15.4, 24.5, 37.4, 38.0, 129.8, 137.1, 145.8, 165.0, 183.5 ppm. M.p. 193 °C.

Crystal structure determinations: CCDC 665303, 665304, 665305, 665306, and 665307 contain the supplementary crystallographic data for this paper. These data can be obtained free of charge from The Cambridge Crystallographic Data Centre via www.ccdc.cam.ac.uk/data_request/cif. For all structures: aryl hydrogen atoms were located and refined isotropically whereas butyl hydrogen atoms were placed on calculated positions and refined in a riding mode.

[(Cp^{BIG})$_2$Ca]: Measurement at −70 °C ($Mo_{K\alpha}$), formula $C_{110}H_{130}Ca$, triclinic, space group $P\bar{1}$, a = 13.0492(5), b = 13.9992(3), c = 14.2958(3) Å, α = 117.808(1), β = 97.666(1), γ = 93.433(1)°, V = 2267.0(1) Å^3, Z = 1, ρ_{calcd} = 1.093 g cm^{-3}, μ ($Mo_{K\alpha}$) = 0.116 mm^{-1}, 205 883 measured reflections, 18 652 independent reflections (R_{int} = 0.043), 14 568 reflections observed with $I > 2\sigma(I)$, θ_{max} = 34.2°, R = 0.0554, $wR2$ = 0.1639, GOF = 1.01, 567 parameters, min/max residual electron density −0.31/+0.41 e Å^{-3}.

[(Cp^{BIG})$_2$Yb]: Measurement at −70 °C ($Mo_{K\alpha}$), formula $C_{110}H_{130}Yb$, triclinic, space group $P\bar{1}$, a = 13.0726(17), b = 14.0196(9), c = 14.3134(9) Å, α = 117.630(3), β = 98.022(4), γ = 93.349(4)°, V = 2278.6(4) Å^3, Z = 1, ρ_{calcd} = 1.184 g cm^{-3}, μ ($Mo_{K\alpha}$) = 1.073 mm^{-1}, 42 543 measured reflections, 10 454 independent reflections (R_{int} = 0.027), 8935 reflections observed with $I > 2\sigma(I)$, θ_{max} = 27.6°, R = 0.0311, $wR2$ = 0.0829, GOF = 1.02, 567 parameters, min/max residual electron density −0.79/+0.49 e Å^{-3}.

[(Cp^{BIG})$_2$Sm]: measurement at −100 °C ($Mo_{K\alpha}$), formula $C_{110}H_{130}Sm$, triclinic, space group $P\bar{1}$, a = 13.0836(11), b = 13.8421(12), c = 14.2398(10) Å, α = 117.488(4), β = 97.117(4), γ = 94.389(4)°, V = 2243.8(3) Å^3, Z = 1, ρ_{calcd} = 1.186 g cm^{-3}, μ ($Mo_{K\alpha}$) = 0.702 mm^{-1}, 39 262 measured reflections, 10 247 independent reflections (R_{int} = 0.025), 5006 reflections observed with $I > 2\sigma(I)$, θ_{max} = 27.5°, R = 0.0301, $wR2$ = 0.0612, GOF = 0.82, 567 parameters, min/max residual electron density −0.87/+0.29 e Å^{-3}.

Received: October 29, 2007
Published online: February 6, 2008

Keywords: calcium · lanthanides · metallocenes · redox chemistry · steric hindrance

[1] a) C. Janiak, H. Schumann, *Adv. Organomet. Chem.* **1991**, *33*, 291; b) R. H. Lowack, K. P. C. Vollhardt, *J. Organomet. Chem.* **1994**, *476*, 25.
[2] M. J. Heeg, C. Janiak, J. J. Zuckerman, *J. Am. Chem. Soc.* **1984**, *106*, 4259.
[3] A. Schott, H. Schott, G. Wilke, J. Brandt, H. Hoberg, E. G. Hoffmann, *Justus Liebigs Ann. Chem.* **1973**, 508.
[4] K. N. Brown, L. D. Field, P. A. Lay, C. M. Lindell, A. F. Masters, *J. Chem. Soc. Chem. Commun.* **1990**, 408.
[5] L. D. Field, T. W. Hambley, P. A. Humphrey, A. F. Masters, P. Turner, *Inorg. Chem.* **2002**, *41*, 4618.
[6] H. Schumann, A. Lentz, R. Weimann, J. Pickardt, *Angew. Chem.* **1994**, *106*, 1827; *Angew. Chem. Int. Ed. Engl.* **1994**, *33*, 1731.
[7] J. C. Ruble, H. A. Latham, G. C. Fu, *J. Am. Chem. Soc.* **1997**, *119*, 1492.
[8] H. Mahomed, A. Bollmann, J. T. Dixon, V. Gokul, L. Griesel, C. Grove, F. Hess, H. Maumela, L. Pepler, *Appl. Catal. A* **2003**, *255*, 355.
[9] a) S. Harder, F. Feil, K. Knoll, *Angew. Chem.* **2001**, *113*, 4391; *Angew. Chem. Int. Ed.* **2001**, *40*, 4261; b) S. Arndt, J. Okuda, *Chem. Rev.* **2002**, *102*, 1953.
[10] Original preparation: a) H. Schumann, A. Lentz, *Z. Naturforsch. B* **1994**, *49*, 1717; b) General one-pot procedure for Ar_5C_5H: G.

Dyker, J. Heiermann, M. Miura, J. I. Inoh, S. Pivsa-Art, T. Satoh, M. Nomura, *Chem. Eur. J.* **2000**, *6*, 3426.
[11] In contrast, reaction of [Cp*$_2$Ca] and [(2-Me$_2$N-α-Me$_3$Si-benzyl)$_2$(thf)$_2$Ca] in benzene gave exclusively the heteroleptic complex [(Cp*)(2-Me$_2$N-α-Me$_3$Si-benzyl)(thf)Ca].
[12] L. R. Morss, *Chem. Rev.* **1976**, *76*, 827.
[13] a) T. D. Tilley, R. A. Andersen, B. Spencer, H. Ruben, A. Zalkin, D. H. Templeton, *Inorg. Chem.* **1980**, *19*, 2999; b) L. Arnaudet, B. Ban, *New J. Chem.* **1988**, *12*, 201; c) H. Sitzmann, T. Dezember, O. Schmitt, F. Weber, G. Wolmershäuser, *Z. Anorg. Allg. Chem.* **2000**, *626*, 2241.
[14] H. A. Zinnen, J. J. Pluth, W. J. Evans, *J. Chem. Soc. Chem. Commun.* **1980**, 810.
[15] E. Sheng, S. Zhou, S. Wang, G. Yang, Y. Wu, Y. Feng, L. Mao, Z. Huang, *Eur. J. Inorg. Chem.* **2004**, 2923.
[16] R. D. Shannon, *Acta Crystallogr. Sect. A* **1976**, *32*, 751.
[17] a) H. B. Kagan, J. Collin, J. L. Namy, C. Bied, F. Dallemer, A. Lebrun, *J. Alloys Compd.* **1993**, *192*, 191; b) V. Nair, A. Deepthi, *Chem. Rev.* **2007**, *107*, 1862.
[18] W. J. Evans, T. A. Ulibarri, J. W. Ziller, *J. Am. Chem. Soc.* **1988**, *110*, 6877.
[19] W. J. Evans, *Inorg. Chem.* **2007**, *46*, 3435.
[20] W. J. Evans, S. L. Gonzales, J. W. Ziller, *J. Am. Chem. Soc.* **1991**, *113*, 1423.
[21] W. J. Evans, K. J. Forestal, J. W. Ziller, *J. Am. Chem. Soc.* **1998**, *120*, 9273.
[22] M. C. Cassani, Y. K. Gun'ko, P. B. Hitchcock, A. G. Hulkes, A. V. Khvostov, M. F. Lappert, A. V. Protchenko, *J. Organomet. Chem.* **2002**, *647*, 71.
[23] W.-Y. Yeh, C.-L. Ho, M. Y. Chiang, I.-T. Chen, *Organometallics* **1997**, *16*, 2698.
[24] W. J. Evans, J. M. Perotti, S. A. Kozimor, T. M. Champagne, B. L. Davis, G. W. Nyce, C. H. Fujimoto, R. D. Clark, M. A. Johnston, J. W. Ziller, *Organometallics* **2005**, *24*, 3916.
[25] a) R. A. Andersen, J. M. Boncella, C. J. Burns, R. Blom, A. Haaland, H. V. Volden, *J. Organomet. Chem.* **1986**, *312*, C49; b) R. A. Williams, T. P. Hanusa, J. C. Huffman, *Organometallics* **1990**, *9*, 1128; c) M. Kaupp, P. von R. Schleyer, M. Dolg, H. Stoll, *J. Am. Chem. Soc.* **1992**, *114*, 8202; d) T. K. Hollis, J. K. Burdett, B. Bosnich, *Organometallics* **1993**, *12*, 3385; e) T. P. Hanusa, *Organometallics* **2002**, *21*, 2559; f) M. Schultz, C. J. Burns, D. J. Schwartz, R. A. Andersen, *Organometallics* **2002**, *21*, 2559; g) W. J. Evans, L. A. Hughes, T. P. Hanusa, *J. Am. Chem. Soc.* **1984**, *106*, 4270.
[26] C. Eaborn, S. A. Hawkes, P. B. Hitchcock, J. D. Smith, *Chem. Commun.* **1997**, 1961.
[27] The electronic effects in the Cp* and Ph_5C_5 ligands are opposite: the latter ligand is able to delocalize negative charge in the Ph rings.
[28] C. M. Forsyth, G. B. Deacon, L. D. Field, C. Jones, P. C. Junk, D. L. Kay, A. F. Masters, A. F. Richards, *Chem. Commun.* **2006**, 1003.
[29] After submission of this manuscript, we presented these results on the Terrae Rarae in Bonn (November 29, 2007) and learned that G. B. Deacon crystallographically characterized [(Ph$_5$C$_5$)$_2$Yb]. The Cp−Yb distance in this metallocene is similar to that in [(Cp^{BIG})$_2$Yb].
[30] In crystal structures determined with X-ray diffraction, observed and refined hydrogen positions always show relatively large errors and are systematically too short. For comparison, hydrogen atoms have been placed at 1.08 Å from the C nucleus (the average C–H bond length) at idealized angles. The C–H bond lengths are hardly influenced by the C–H···C(π) interaction. See also reference [31e].
[31] a) R. Hunter, R. H. Haueisen, A. Irving, *Angew. Chem.* **1994**, *106*, 588; *Angew. Chem. Int. Ed. Engl.* **1994**, *33*, 566; b) T. Steiner, *J. Chem. Soc. Chem. Commun.* **1995**, 95; c) T. Steiner, M. Tamm, A. Grzegorzewski, N. Schulte, N. Veldman, A. M. M. Schreurs, J. A. Kanters, J. Kroon, J. van der Maas, B. Lutz, *J. Chem. Soc. Perkin Trans. 2* **1996**, 2441; d) G. R. Desiraju, *Chem. Commun.* **2005**, 2995; e) S. Harder, *Chem. Eur. J.* **1999**, *5*, 1852.
[32] a) G. Karlström, P. Linse, A. Wallquist, B. Jönsson, *J. Am. Chem. Soc.* **1990**, *112*, 4768; b) J. M. Steed, F. A. Dixon, W. Klemperer, *J. Chem. Phys.* **1979**, *70*, 4940; c) G. J. Piermarini, A. D. Mighell, C. E. Weir, S. Block, *Science* **1969**, *165*, 1250.
[33] D. Mootz, A. Deeg, *J. Am. Chem. Soc.* **1992**, *114*, 5887.
[34] a) A. Karpfen, *Adv. Chem. Phys.* **2002**, *123*, 469; b) G. R. Desiraju, T. Steiner, *The Weak Hydrogen Bond*, Oxford University Press, New York, **1997**.
[35] L. D. Field, T. W. Hambley, T. He, P. A. Humphrey, C. M. Lindall, A. F. Masters, *Aust. J. Chem.* **1996**, *49*, 889.
[36] L. D. Field, T. W. Hambley, T. He, A. F. Masters, P. Turner, *Aust. J. Chem.* **1997**, *50*, 1035.
[37] W.-Y. Yeh, S.-M. Peng, G.-H. Lee, *J. Organomet. Chem.* **1999**, *572*, 125.
[38] S. Harder, S. Müller, E. Hübner, *Organometallics* **2004**, *23*, 178.
[39] S. Harder, F. Feil, *Organometallics* **2002**, *21*, 2268.
[40] S. Harder, *Organometallics* **2005**, *24*, 373.
[41] The crystal structures of [(2-Me$_2$N-benzyl)$_3$Yb] and [(2-Me$_2$N-benzyl)$_3$Sm] have been determined and will be discussed in a forthcoming paper. Crystal data for [(2-Me$_2$N-benzyl)$_3$Yb]: measurement at −70 °C ($Mo_{K\alpha}$), formula $C_{27}H_{36}N_3Yb$, monoclinic, space group $P2_1/c$, $a = 16.8969(5)$, $b = 9.4642(3)$, $c = 16.6694(5)$ Å, $\beta = 111.297(2)°$, $V = 2483.7(1)$ Å^3, $Z = 4$, $\rho_{calcd} = 1.539$ g cm^{-3}. Crystal data for [(2-Me$_2$N-benzyl)$_3$Sm]: measurement at −100 °C ($Mo_{K\alpha}$), formula $C_{27}H_{36}N_3Sm$, monoclinic, space group $P2_1/c$, $a = 16.8989(8)$, $b = 9.4648(7)$, $c = 16.6603(10)$ Å, $\beta = 110.911(3)°$, $V = 2489.2(3)$ Å^3, $Z = 4$, $\rho_{calcd} = 1.475$ g cm^{-3}.

